Pulse train interaction and control in a microcavity laser with delayed optical feedback

SOIZIC TERRIEN[1,*], BERND KRAUSKOPF[1], NEIL G. R. BRODERICK[1], RÉMY BRAIVE[2], GRÉGOIRE BEAUDOIN[2], ISABELLE SAGNES[2], AND SYLVAIN BARBAY[2]

[1] *The Dodd-Walls Centre for Photonic and Quantum Technologies, The University of Auckland, New Zealand*
[2] *Centre de Nanosciences et de Nanotechnologies, C2N-UMR9001, CNRS, Université Paris-Sud, Université Paris-Saclay, Site de Marcoussis, Route de Nozay, 91460 Marcoussis, France*
[*] *Corresponding author: s.terrien@auckland.ac.nz*

Compiled March 2, 2018

We report experimental and theoretical results on the pulse train dynamics in an excitable semiconductor microcavity laser with integrated saturable absorber and delayed optical feedback. We show how short optical control pulses can trigger, erase or retime regenerative pulse trains in the external cavity. Both repulsive and attractive interactions between pulses are observed, and are explained in terms of the internal dynamics of the carriers. A bifurcation analysis of a model consisting of a system of nonlinear delay differential equations shows that arbitrary sequences of coexisting pulse trains are very long transients towards weakly stable periodic solutions with equidistant pulses in the external cavity.

OCIS codes: (190.0190) Nonlinear optics; (140.3538) Lasers, pulsed; (190.1450) Bistability; (190.5530) Pulse propagation and temporal solitons.

http://dx.doi.org/10.1364/ao.XX.XXXXXX

1. INTRODUCTION

Controllable sources of short optical pulse trains are at the heart of many recent developments in physics, with potential applications to optical telecommunications and signal processing. Trains of short pulses can arise from cw, coherently-driven optical fibre cavities [1] or nonlinear microcavities [2, 3], forming dissipative temporal solitons. In the laser regime, mode-locked dissipative solitons have been observed in fibre laser cavities [4] and in a face-to-face VCSEL configuration [5]. Pulse trains can also be produced by using the regenerative self-pulsing configuration of an excitable laser with time-delayed feedback. This configuration was implemented in a coherently driven VCSEL [6], an opto-electronic system [7] and a micropillar laser with integrated saturable absorber [8, 9]. Excitability [10, 11] is associated with an all-or-none response to external perturbations, depending on whether or not the amplitude of the perturbation exceeds the excitability threshold. In the excitable regime, a laser with saturable absorber (LSA) subject to a perturbation either emits an excitable response in the form of a short, high-amplitude pulse, or relaxes back to its off-state [11]. In the presence of an optical feedback loop with delay τ, the reinjection of an initial excitable pulse can trigger another excitable response. As the process repeats, this results in a train of pulses with a repetition rate close to the feedback delay [9]. This picture is however oversimplified, and a theoretical analysis predicts more complicated dynamics, including the coexistence of several self-pulsing modes with the stable off-state [12, 13]. In particular, bistability between a pulsing periodic solution and the off-state is a condition for the on and off switchability of the regenerative pulse trains [9]. The pulsing dynamics is also driven by the nonlinear latency between the reinjection and the regeneration of a pulse [14–16], which is strongly related to the net gain dynamics of the laser active medium accounting for the saturable gain and saturable loss. Despite similar features of the pulsing dynamics, it is worth noting that the physics involved here differs considerably from the one of temporal dissipative solitons in e.g. mode-locked lasers [5]: the micropillar LSA with delayed feedback is intrinsically a single mode system and does not involve the locking dynamics of several external cavity modes.

In this Letter, we present experimental results on the optical control and interaction of pulse trains in an excitable micropillar laser with integrated saturable absorber and delayed optical feedback. We show that the Yamada model with incoherent delayed optical feedback describes the pulsing dynamics in very good agreement with the experiment [9, 11], and allows us to explain the pulse-to-pulse interactions by the carrier dynamics of the laser. We reconcile the bifurcation analysis of the model with the numerical and experimental observations showing that non-regularly timed pulse trains are in fact very long transients, which evolve to solutions with equidistant pulses in the external cavity as a consequence of the carrier dynamics. In constrast to temporal dissipative solitons in other systems [17, 18], we show that pulse trains can also show attractive interactions. Finally, we show that reliable all-optical pulse train control is possible experimentally with short optical control pulses.

2. EXPERIMENTAL SETUP AND MODEL

The experimental setup is similar to the one described in [9], but with improved feedback strength thanks to a considerable reduction of feedback losses. A micropillar laser with integrated

saturable absorber [19, 20] emitting around 980nm is optically pumped at 800nm. The laser emission is fed back after a delay τ through a mirror located several tens of centimeters away. Part of the emitted beam is selected by a beamsplitter and analyzed by a camera and a fast avalanche photodetector (> 5GHz bandwitdh). The solitary micropillar laser is excitable for a large range of pump powers below threshold [11]. The 80ps optical perturbations triggering an excitable response are produced by a mode-locked Ti:Sa laser emitting at ∼800nm.

This system is modelled by the Yamada rate equations with incoherent delayed optical feedback [12, 21]:

$$\begin{aligned} \dot{G} &= \gamma_G(A - G - GI), \\ \dot{Q} &= \gamma_Q(B - Q - aQI), \\ \dot{I} &= (G - Q - 1)I + \kappa I(t - \tau), \end{aligned} \tag{1}$$

for the dimensionless gain G, absorption Q and intensity I. Here, A is the pump parameter, B is the non-saturable absorption, a is the saturation parameter and γ_G and γ_Q are the carrier recombination rates in the gain and absorption media, respectively. The delayed term in the intensity equation describes incoherent feedback with delay τ and strength κ. The parameter values used in simulation are, unless otherwise stated, $A = 2.4$, $B = 2.2$, $\gamma_G = 0.01$, $\gamma_Q = 0.02$, $a = 5$, $\kappa = 0.05$ and $\tau = 1100$. These are chosen both to match the known physical parameters and the experimental observations. The results presented here are robust in the presence of reasonable amounts of both spontaneous emission and pump noise. Hence, we do not include noise terms in (1) and concentrate on the deterministic dynamics.

3. WRITING AND COEXISTENCE OF PULSE TRAINS

Fig. 1 shows a direct comparison between observed and simulated pulse trains. The temporal traces are folded at the delay time τ and stacked vertically in a pseudo-space representation [22]. In panel (a1), a single external perturbation leads, as expected, to a pulse train whose repetition rate is slightly larger than the delay time τ, due to the nonlinear latency time of the excitable response [14, 15]. Pulse trains can be sustained for very long time, depending on the feedback strength and on the amount of noise in the system [9]. For very low feedback losses, the observed pulse train duration is limited by the acquisition memory of the oscilloscope.

In panel (b1), two successive perturbations are sent with a time difference of 12.5ns. This leads to the coexistence of two pulse trains in the cavity, separated by a time interval of approximately $0.4 \times \tau$ which seems to remain constant on the timescale of 250 round trips. This suggests that this pulse train does not correspond to a harmonic regime. Three coexisting pulse trains can also be observed, as in Fig. 1(c1). As shown in Fig. 1(a2)–(c2), these experimental results can be matched almost perfectly by the Yamada model (1).

For the same parameters, Fig. 2 represents the phase portrait of system (1) in the (G, I)-plane, calculated with the continuation toolbox DDE Biftool [23, 24]. It shows the coexistence of seven stable solutions: a non-lasing equilibrium and six periodic pulsing solutions. These coexist with several unstable periodic solutions and equilibria, which are not represented here. The stable pulsing solutions have periods T close to submultiples of τ, and hence correspond to different numbers of equidistant pulses in the external cavity [13]. Apart from the one for which T is close to τ, they all are only weakly stable: the modulus of their leading Floquet multiplier, shown in Fig. 2 (b), is very close to one. Importantly, there exists no stable periodic solutions with non-equidistant pulses in the external cavity, despite the fact that such solutions are observed over long periods of time in experiments and simulations.

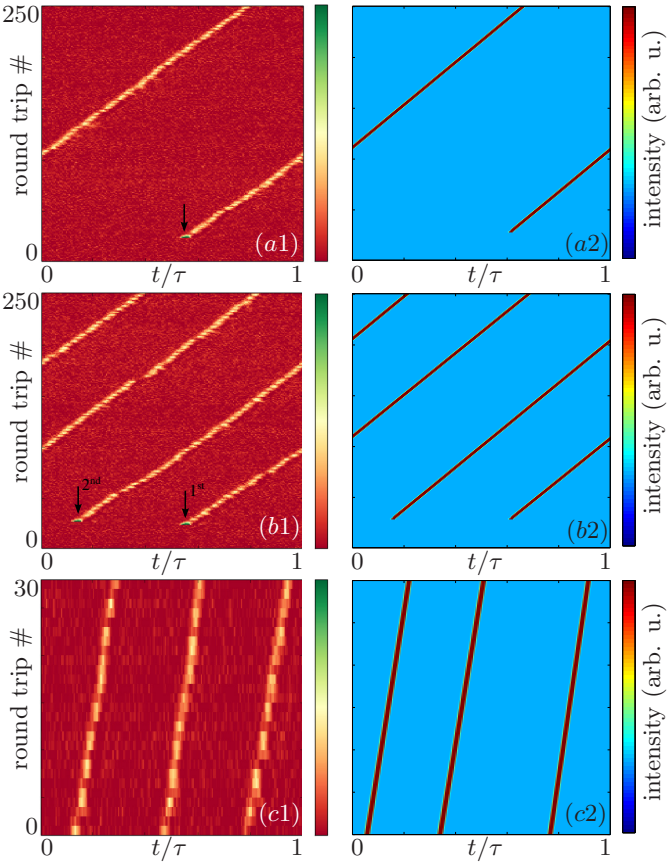

Fig. 1. Pseudo-space representation of experimental (left) and simulated (right) pulse trains following one (a), two (b) and three (c) perturbations. In the experiment, the feedback delay time is 4.77ns.

4. LONG-TERM BEHAVIOUR

This raises the question of the long-term behaviour of pulse trains with non-equidistant pulses (Fig. 1(b)–(c)). Fig. 3(a–c) represents the relative timing of two coexisting pulses of (1) over several hundreds of round trips, showing that the two pulses become equidistant in the long term. In fact, regimes with non equidistant pulses are very long transients toward one of the (weakly) attracting periodic solutions of Fig. 2(a). The bifurcation analysis of equations (1) shows that the amplitudes of the periodic solutions with largest periods are very close to each other (see the two largest orbits in Fig. 2) [13]: as such, no significant difference is observed in the amplitudes when one or several pulses exist in the external cavity.

The slow convergence towards the stable periodic solution is explained entirely by the dynamics of the net gain $\tilde{G} = G - Q - 1$. In the solitary laser, each excitable pulse is followed by an absolute and a relative refractory periods, during which no other pulse can be triggered, or the conditions to trigger another pulse are more stringent, respectively [8]. These time windows are related to the recovery time of the carriers in the

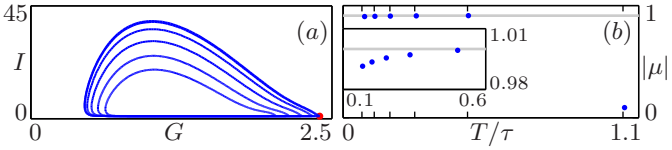

Fig. 2. (a): Phase portrait of (1) in the (G, I)-plane, showing one stable equilibrium (dot) and six stable periodic solutions (curves). (b) Modulus of the leading Floquet multiplier of each periodic solution, with respect to its period.

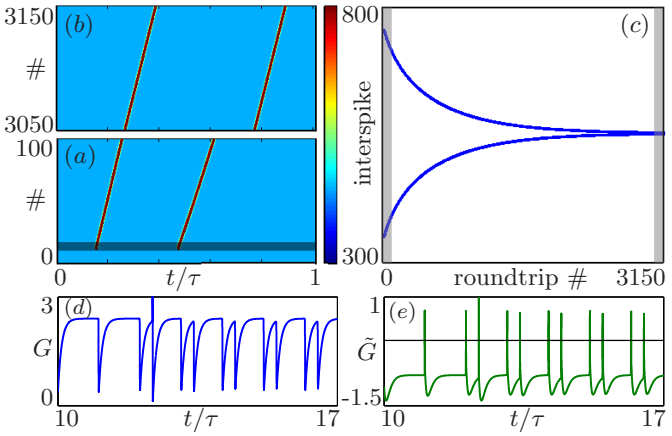

Fig. 3. Simulation of two coexisting pulse trains. (a–b) Pseudo-space representation just after the perturbations and in the long term. (c) Evolution of the elapsed time between successive pulses; the shaded areas are the segments represented in (a) and (b). Temporal evolution in the shaded area of panel (a) of: (d) gain G and (e) net gain $\tilde{G}$.

gain and absorber sections of the microlaser, described by γ_G and γ_Q. In Fig. 3(d–e), the absorption recovers faster than the gain ($\gamma_Q > \gamma_G$): after a pulse, the low net gain $\tilde{G}$ increases back to its saturated value as the gain G recovers. The second perturbation is introduced in the relative refractory period of the first pulse, where the absorber recovered entirely, and the gain has recovered sufficiently for the second pulse to be sustained. However, it did not recover entirely, so that the net gain experienced by the second pulse train is slightly smaller than for the first pulse train. Because the net gain determines the latency of the excitable response to a perturbation [15], this results in a slightly larger response time, and hence repetition period, for the second pulse train compared to the first pulse train. Round trip after round trip, the second pulse is reinjected further away from the first one, until both pulse trains experience an identical net gain, and their repetition periods become equal. This convergence to the solution with equidistant pulses gives the impression of a repulsion between pulses.

Because the system converges in the long term to a stable periodic orbit of the phase portrait, the maximum number of pulses that can be sustained simultaneously is related to the number of stable periodic solutions. In Fig. 2, the periodic orbit with the smallest period corresponds to the coexistence of six pulses in the external cavity. In Fig. 4(a), six pulse trains are triggered and indeed sustained in simulation, and they become equidistant after several round trips. Three different scenarios can result from a seventh perturbation, depending on its timing. When sent in the absolute refractory period of an existing pulse,

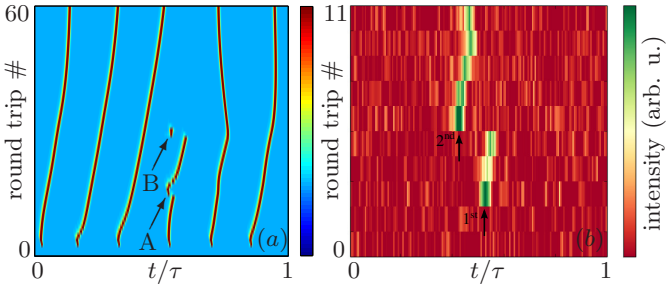

Fig. 4. (a) Simulated pulse trains following six perturbations, and effect of a seventh perturbation for two different timing (A and B). (b) Experimental retiming of a pulse train.

the low gain prevents a pulse from being triggered. If sent just before an existing pulse (case A), a new pulse is triggered but the absolute refractory period of the newly created pulse prevents the next pre-existing pulse to be regenerated. This results in the *retiming* of the pulse train while keeping the number of coexisting pulses unchanged; see also the experimental plot in Fig. 4(b). When the seventh perturbation is sent in the relative refractory period of a pre-existing pulse (case B), the gain G did not recover entirely, and the newly created pulse thus has a small amplitude, which prevents its regeneration after a delay τ. Moreover, the absolute refractory period of this single pulse results in a switch off by preventing the regeneration of the next pulse. The final state has only five coexisting pulses, which then converge towards an equidistant configuration. Overall, there is no suitable perturbation timing to trigger a sustained seventh pulse. From a mathematical point of view, these different scenarios are related to the basins of attraction of the different stable periodic solutions. The ability of a perturbation to bring the system outside of the basin of a periodic orbit obviously depends on both amplitude and timing along the orbit. A detailed study of these basins is beyond the scope of this Letter, and will be discussed elsewhere.

5. PULSE TRAINS INTERACTION

We showed the existence of a weak "repulsion" of a second pulse in Fig. 3. More surprisingly, "attractive" interaction is also observed, as shown in Fig. 5(a)–(b) for experimental and simulated data. The explanation of this phenomenon is more subtle and now requires consideration of the dynamics of both the net gain $\tilde{G}$ and the gain G. Here, γ_G must be larger than γ_Q, so that the net gain $\tilde{G}$ decreases in between two pulses, as shown in Fig. 5(c). The second perturbation is introduced in the relative refractory period of the first pulse, where it benefits from a higher net gain than the first pulse train. The response time of the laser is thus shorter, which results in a slightly smaller repetition rate for the second pulse train compared to the first one. Round trip after round trip, the second pulse is reinjected closer and closer to the first pulse and benefits from a higher and higher net gain, which shortens further the repetition rate and explains the impression of an attraction between the pulses. Eventually, the second pulse is reinjected when insufficient gain G is available, which prevents its regeneration and stops the second pulse train.

The pseudo-space representation in Fig. 3–5 may suggest that the pulses interact in the external cavity. However, we stress that the only mechanism for interaction is through the gain and absorption in the microlaser itself. Although the systems are

fundamentally different, a similar mechanism was suggested in [25] for a model for mode-locked lasers, that explains the stability properties of mode-locked solutions with one and several pulses in the laser cavity. However, to our best knowledge, attractive interaction has never been observed.

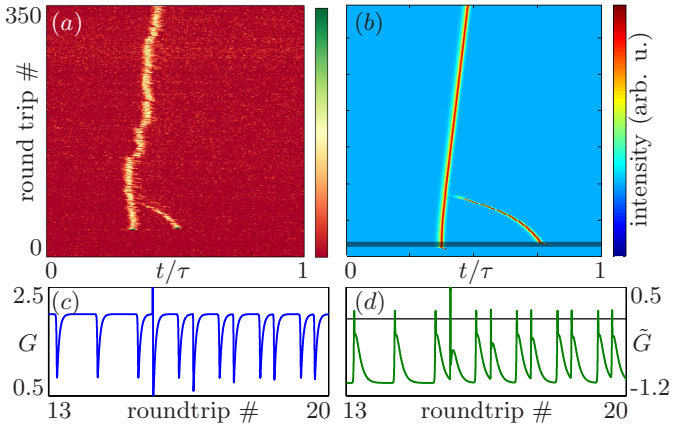

Fig. 5. (a) and (b) Attractive interaction between two experimental and simulated pulse trains. (c) and (d) Temporal evolution of G and $\tilde{G}$ in the shaded area of panel (b). In simulation, the parameters are $A = 2$, $B = 2$, $\gamma_G = 0.02$, $\gamma_Q = 0.01$, $a = 10$, $\kappa = 0.1$ and $\tau = 1000$.

6. OPTICAL CONTROL OF PULSE TRAIN DURATION

Based on these mechanisms, we show that a short optical external perturbation can reliably switch on and off a pulse train. This is much faster than existing techniques; in particular, it does not involve a modulation of the pumping current or a precise control of the phase of the holding beam [17, 18]. Fig. 6(a) shows two successive perturbations, and the resulting experimental temporal trace is Fig. 6(b). The pulse train is reliably switched off by the second perturbation, which has been checked for one thousand experimental realisations. There is a definite window in the amplitude and timing of the second perturbation to switch off the pulse train. In particular, the two perturbations are sent 12.5 ns apart for technical reasons, but the feedback delay (4.2ns) is chosen such that the second perturbation arrives just before the regeneration of the fourth pulse. This phenomenon can be reproduced in the model, which requires a careful choice of parameter values, so that a second perturbation brings the system into the basin of attraction of the off-state.

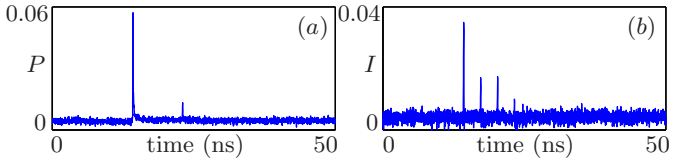

Fig. 6. (a) External perturbations and (b) response of the experimental device.

7. CONCLUSION

We have shown that an excitable micropillar laser with delayed optical feedback can sustain several pulse trains in the external cavity, which can be reliably and independently controlled all-optically by short pulses. By using a suitable mathematical model, we show that all pulsing dynamics are long transients towards a periodic solution with equidistant pulses in the external cavity. The impression of attractive and repulsive pulse interactions is explained entirely by latencies generated by the gain and net gain dynamics in the microlaser itself. As such, this interaction mechanism does not involve the notion of force. Rather, the only ingredients needed are excitability and self-feedback. These are encountered in many systems, including neurons and cardiac cells [10]. As such, our results might be applicable to systems beyond the particular device considered here.

REFERENCES

1. F. Leo, S. Coen, P. Kockaert, S.-P. Gorza, P. Emplit, and M. Haelterman, Nat Photon **4**, 471 (2010).
2. T. Herr, V. Brasch, J. D. Jost, C. Y. Wang, N. M. Kondratiev, M. L. Gorodetsky, and T. J. Kippenberg, Nat Photon **8**, 145 (2014).
3. A. M. Weiner, Nat Photon **11**, 533 (2017).
4. P. Grelu and N. Akhmediev, Nat. Photonics **6**, 84 (2012).
5. M. Marconi, J. Javaloyes, S. Balle, and M. Giudici, Phys. Rev. Lett. **112**, 223901 (2014).
6. B. Garbin, J. Javaloyes, G. Tissoni, and S. Barland, Nat Commun **6**, (2015).
7. B. Romeira, R. Avó, J. M. L. Figueiredo, S. Barland, and J. Javaloyes, Sci. reports **6** (2016).
8. F. Selmi, R. Braive, G. Beaudoin, I. Sagnes, R. Kuszelewicz, and S. Barbay, Phys. Rev. Lett. **112**, 183902 (2014).
9. S. Terrien, B. Krauskopf, N. G. R. Broderick, L. Andréoli, F. Selmi, R. Braive, G. Beaudoin, I. Sagnes, and S. Barbay, Phys. Rev. A **96** (2017).
10. E. M. Izhikevich, *Dynamical systems in neuroscience* (MIT press, 2007).
11. S. Barbay, R. Kuszelewicz, and A. M. Yacomotti, Opt. Lett. **36**, 4476 (2011).
12. B. Krauskopf and J. J. Walker, *Bifurcation Study of a Semiconductor Laser with Saturable Absorber and Delayed Optical Feedback* (Wiley-VCH Verlag GmbH & Co. KGaA, 2012), pp. 161–181.
13. S. Terrien, B. Krauskopf, and N. G. R. Broderick, SIAM J. for Appl. Dyn. Syst. **16**, 771 (2017).
14. J. L. A. Dubbeldam, B. Krauskopf, and D. Lenstra, Phys. Rev. E **60**, 6580 (1999).
15. F. Selmi, R. Braive, G. Beaudoin, I. Sagnes, R. Kuszelewicz, T. Erneux, and S. Barbay, Phys. Rev. E **94**, 042219 (2016).
16. T. Erneux and S. Barbay, "Analytical studies of an excitable micropillar laser with a saturable absorber," Submitted (2017).
17. J. K. Jang, M. Erkintalo, S. Coen, and S. G. Murdoch, Nat. communications **6**, 7370 (2015).
18. P. Camelin, J. Javaloyes, M. Marconi, and M. Giudici, Phys. Rev. A **94**, 063854 (2016).
19. S. Barbay, Y. Ménesguen, I. Sagnes, and R. Kuszelewicz, Appl. Phys. Lett. **86**, 151119 (2005).
20. T. Elsass, K. Gauthron, G. Beaudoin, I. Sagnes, R. Kuszelewicz, and S. Barbay, Eur. Phys. J. D **59**, 91 (2010). 10.1140/epjd/e2010-00079-6.
21. M. Yamada, Quantum Electron. IEEE J. **29**, 1330 (1993).
22. G. Giacomelli and A. Politi, Phys. D: Nonlinear Phenom. **117**, 26 (1998).
23. K. Engelborghs, T. Luzyanina, and G. Samaey, Tech. rep., Department of Computer Science, KU Leuven, Leuven, Belgium (2001).
24. J. Sieber, K. Engelborghs, T. Luzyanina, G. Samaey, and D. Roose, Tech. rep., http://arxiv.org/abs/ 1406.7144 (2015).
25. M. Nizette, D. Rachinskii, A. Vladimirov, and M. Wolfrum, Phys. D: Nonlinear Phenom. **218**, 95 (2006).